

AN INTELLIGENT EDUCATIONAL SYSTEM FOR HELPING RAPID DETECTION OF COVID-19 TO REDUCE THE SPREAD OF INFECTION

Faten Abd El-Sattar Zahran El-Mougi

M. Hussein*

Computer Science Department, Faculty of Specific
Education, Mansoura University
Mansoura, Egypt

faten_com1@mans.edu.eg

Computer Science Department, Faculty of Specific
Education, Mansoura University
Mansoura, Egypt

marwahussien@mans.edu.eg

Received 2024-08-30; Revised 2024-10-02; Accepted 2024-10-05

Abstract. COVID-19 is considered a significant global health concern due to its high human-to-human transmission, leading to an increase in the number of infections and fatalities. Hence, the prevention of COVID-19 transmission and the reduction of mortality rates are contingent on the early detection of the disease. This study proposes an intelligent educational system which based on artificial intelligence techniques to assist doctors in medical educational institutions in the rapid detection of suspected instances of COVID-19 for preventing the virus from spreading. The system integrates three main components for quick detection and reducing infection spread. The first part involves diagnosis based on radiological images (chest X-Ray), the second part relies on medical analysis laboratory data, and the third part considers diagnosing based on crucial symptoms indicating the potential infection with coronavirus disease. The results from these three parts are combined to obtain the final diagnosis decision using a convolutional neural network (CNN) approach for chest X-ray image identification, the study demonstrates that the proposed method aligns closely with expert diagnoses, indicating high accuracy with 0.97%, and speed in identifying probable COVID-19 cases.

Key-words: Artificial Intelligence; COVID-19; Chest X-ray; CNN; Pneumonia.

1. Introduction

The coronavirus epidemic that occurred in Wuhan, China in 2019 affected the whole world. The disease caused by this virus was referred to in the literature as COVID-19. COVID-19, a highly contagious infection, spreads rapidly, especially through droplets and direct contact. In symptomatic cases, fever, exhaustion, muscle soreness, sore throat, and dry cough are the most frequent symptoms. The Covid-19 epidemic claimed the lives of 3 million people globally in April 2021, according to the most recent world health organization (WHO) data. [1]. In COVID-19 pneumonia, early diagnosis and isolation are

*Corresponding Author: Marwa Hussien

Computer Science Department, Faculty of Specific Education, Mansoura University, Mansoura, Egypt

Email address: marwahussien@mans.edu.eg

the main parameters in preventing the spread of the disease. It is also very important for the early treatment of the patient. It is essential to know the treatment methods well to prevent contamination especially during the incubation period. Patients with Covid-19 are diagnosed via reverse transcriptase polymerase chain reaction (RT-PCR) tests, or real-time polymerase chain reaction. This test is a very important parameter in detecting the virus. Although it is a very important test for diagnosis, obtaining the clinical results of Covid-19 patients with this method is quite time-consuming. In cases where RT-PCR results are negative and show symptoms, radiological data are usually guiding. In contrast, RT-PCR tests have also been found to produce false negative findings or fluctuating results in the diagnosis of COVID-19 cases [2]. In order to prioritize and properly treat patients with respiratory symptoms, quick detection of COVID-19 in hospitals is essential. RT-PCR is the most sophisticated technique for verifying a suspected COVID-19 case. The PCR process, however, takes a long time, and some studies have shown that its sensitivity is only about 90.7%. [3]. Software developers and experts in the field have created advanced instruments to assist medical practitioners in making judgments as computer technology has improved [4].

The COVID-19 outbreak stands out as one of the most serious public health issues in recent memory. The virus exhibits rapid transmission, with an initial reproduction number ranging from 2.24 to 3.58 during the early stages of the pandemic. This indicates that, on average, each infected individual transmitted the disease to two or more other people [5]. Clinical decision support systems are software tools that support medical professionals in their decision-making and demonstrate the power of sophisticated reasoning to enhance clinical judgment, ultimately promoting more efficient medical procedures. By using expert systems to program computers with rules that would allow them to "think" like expert doctors instead of patients, researchers created them [6]. As well as other basic symptoms like fever, cold, body aches, sore throat, and epistaxis, pneumonia appears to be the most typical sign of contamination for COVID-19. Many nations have declared total lock-down and instructed their citizens to stay indoors and strictly avoid gatherings [7]. In its most severe forms, COVID-19 affects the lungs, which can cause pneumonia. If the lung is affected by bacterial, viral, or COVID-19 pneumonia, radiographic evaluation of the lungs, such as a chest X-ray, CT scan, ultrasonography, and other imaging modalities, can be utilized to determine this [8]. RT-PCR testing can also be used to diagnose COVID-19 using traditional laboratory methods. The RT-PCR takes longer and might often produce false negative results [9]. Fortunately, radiographic pictures of the lungs can be immediately used to detect COVID-19 infection. This may result in an early isolation of the affected person, stopping the spread of the disease. However, if the virus has not yet penetrated the lungs, radiological imaging will not be of any use. Because it obtains samples from the nose or throat, where the virus initially assembles and spreads, RT-PCR performs well in such circumstance [10]. Using visual scanning, radiologists must search for ground-glass opacity (GGO) in the lungs to establish COVID-19. Therefore, machine learning (ML) is required to provide an automatic identification approach as a fast alternative diagnosis option and stop the human transmission of COVID-19. Numerous studies have sought to use magnetic resonance (MR) pictures to detect various diseases, such as brain tumors, as well as X-ray images to detect pulmonary ailments, such as pneumonia [11].

2. Related Work

In order to distinguish COVID-19 patients from healthy patients, Ahmed developed Deep-COVID-19, a straightforward CNN architecture that outperformed the relevant models VGG16, VGG19, and Mobile Nets with 95% accuracy. His work also presented a critical assessment of three commercial CNN architectures that were initially proposed for natural image processing to be able to help radiologists differentiate COVID-19 disease due to other diseases according to chest X-ray images [12]. Aijaz et al.

proposed a deep CNN architecture for COVID-19 diagnosis according to classification chest X-ray images. The evaluation outcomes revealed a 99.5% total accuracy rate, confirming the CNN model's great competency in the application area[13]. With the goal of quickly identifying patients who were infected and accelerating the diagnostic procedure, Zaneer et al. used a CNN-based transfer learning algorithm to use chest X-ray images from three different open-source datasets to identify coronavirus phenomena. In three separate instances, they also changed the CNN design to enhance the classification outcomes. The experimental findings demonstrated excellent COVID-19 detection performance[14]. In order to counteract this epidemic, Faisal et al. offered a thorough analysis of AI-enabled techniques that employ medical pictures. The main goal of that survey was to portray the most recent data so that researchers could comprehend and be aware of the most recent findings and develop a model that could accurately diagnose COVID-19 disease at a reasonable cost and relatively faster. They also noted that domain adoption in transfer learning, a commonly utilized method that produced encouraging results[15]. Linda et al. introduced COVIDNet, a deep convolutional neural network design created exclusively for the detection of COVID-19 instances from chest X-ray images. The broader public can access it because it is open source. They looked into the explainability method used by COVID-Net to make predictions in an effort to better understand COVID cases' key components so that clinicians can conduct more effective screening and foster greater trust and transparency when using COVID-Net for expedited computer-aided screening[16].

Through the previous studies, some of them relied in its discovery of suspected cases of infection with COVID-19 on the use of only one method or two together at most; some of them depended on x-ray images or CT scans only, or symptoms only, or medical analysis laboratory data only, and the other studies depended on combining x-ray images with symptoms, or combining medical analysis laboratory data with x-ray images. From these observations; the proposed system became more unique, effective and accurate system. It combined the three methods in the rapid detection of suspected cases of infection with the COVID-19. We provide a method based on deep learning for detecting COVID-19 infections from chest X-ray images. CNN model is what we suggest for the classification of normal, pneumonia, lung opacity, and the four major forms of COVID-19. With data from other studies in the literature, we compared the findings. The suggested system will assist us in determining how the four categories differ from one another and what makes COVID-19 unique compared to other illnesses. The triage, quantification, and follow-up of positive cases will be greatly aided by a model that can detect COVID-19 infection from chest x-ray images. Even though it has not entirely change the current testing technique, this model can be utilized to decrease the number of cases that need urgent testing or additional review.

3. The Proposed Approach

The suggested system consists of three essential components: The first part, the diagnosing based on radiological images chest X-Ray. The second part, the diagnosing based on medical analysis laboratory data. And the third part, the diagnosing based on the most important symptoms that indicate the possibility of infection with coronavirus disease. Fig. 1 shows the proposed system's structure.

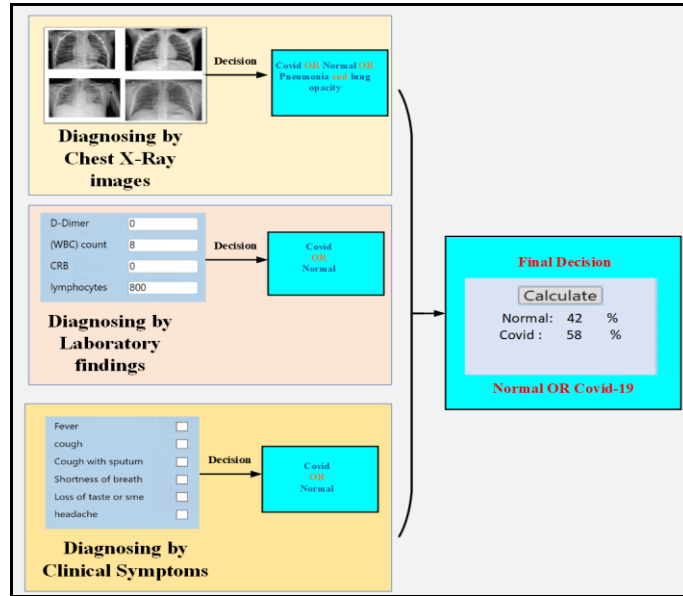














Fig. 1 The proposed system's structure

3.1. Diagnosing Based on Chest X-ray Images

3.1.1 Material and Methods

This step aims to classify COVID-19, normal, pneumonia, and lung opacity cases using CNN model. The datasets collected from the open-source Kaggle[17-19] . It consists of 9335 chest x-ray image, 2425 COVID-19, 2220 normal, 2305 pneumonia, and 2385 lung opacity. It splitted into 80% as training and 20% as testing set. Table 1 shows samples of chest x-ray images (normal, COVID-19, pneumonia, and lung opacity). Fig. 2 shows the flowchart for the main steps of diagnosing based on chest x-ray images in the suggested system using CNN model.

Table 1 Samples of chest x-ray images (normal, COVID-19, pneumonia, and lung opacity)

Images			Class Name
			normal
			COVID-19
			pneumonia
			lung opacity

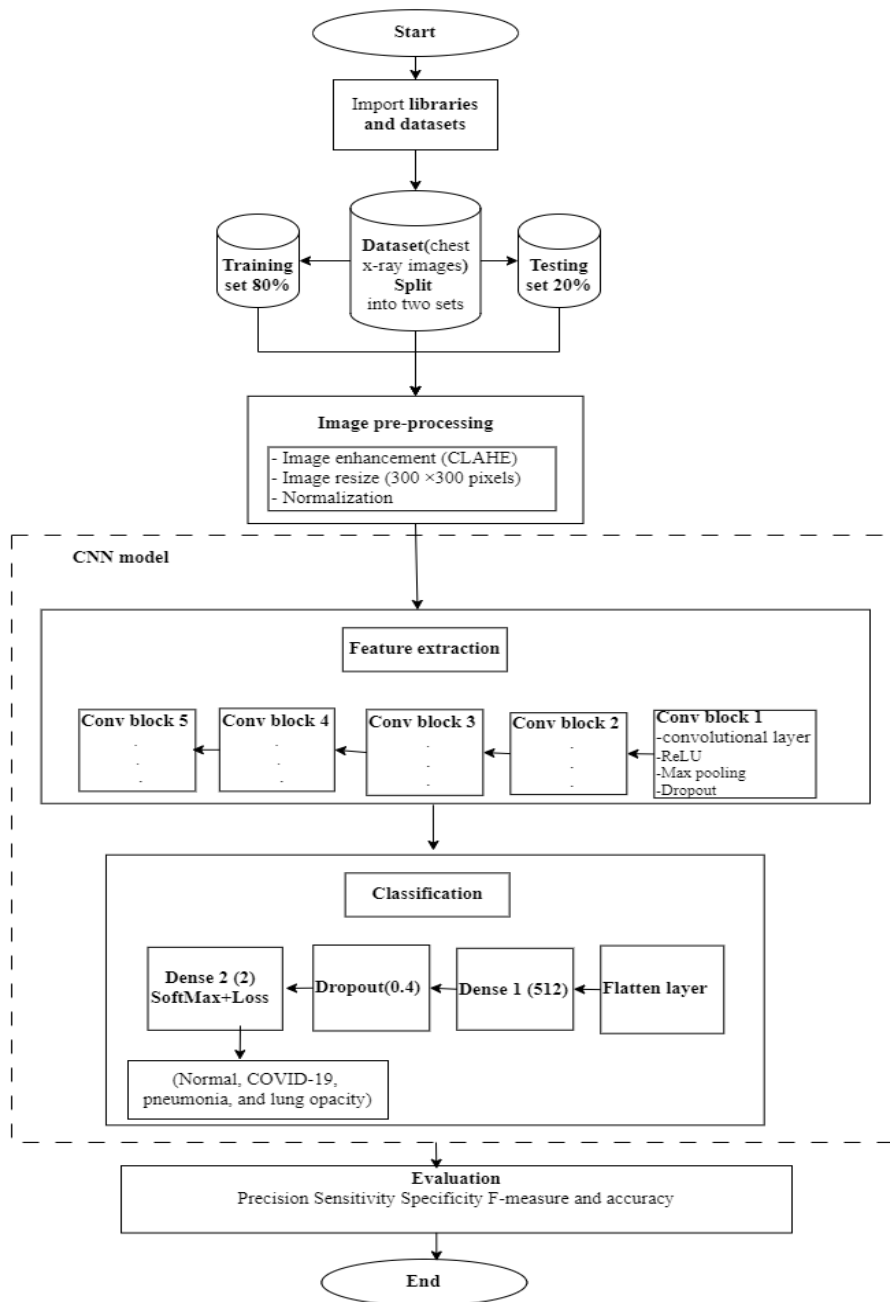


Fig. 2The flowchart for the main steps of diagnosing based on chest x-ray images using CNN model.

A) Pre-processing stage

In pre-processing we prepare the data for the feature extraction stage which comes after; to enhance the model's accuracy. This stage contains three steps: resizing chest x-ray images, applying contrast limited adaptive histogram equalization (CLAHE) technology to improve them, and normalization.

- Resizing chest x-ray images

To effectively accommodate the processing in deep learning systems, the loading of all chest x-ray images for scaling at a set size of (300×300) pixel. The chest x-ray scans are resized to a (300×300) pixel scale in this stage, which lowers the computing cost because it increases processing effectiveness.

- Chest x-ray images enhancement CLAHE

The CLAHE technique is used in this stage to pre-process the chest x-ray scanning image. This method of contrast enhancement effectively increases contrast, removes noise and blurring, sharpens features, and reveals image information (such edge and boundary detection) despite altering the chest x-ray image's basic structure. The primary concept behind this technique is to first separate the input image into tiles, which are discrete pieces of equal and non-overlapping sizes. The histogram is then calculated for each component because this method relies on the local histogram rather than the global histogram. The histogram is then clipped at predetermined levels to address the noise over-amplification issue, and it is periodically distributed to other tiles before the cumulative distributing technique is computed. The cumulative histogram is then used to determine the equalization. The two parameters employed by the CLAHE technique are the clip limit (CL), which specifies noise amplification, and the number of tiles (NT), which specifies the quantity of non-overlapping sub-regions.[20].

- Chest x-ray images Normalization

The same patient may receive X-ray images that look very differently from different X-ray device manufacturers. In computer-aided diagnostic devices, over fitting to the device's pixel distributions is a significant issue, hence contrast normalization is typically used to reduce this issue. The goal is to uniformly distribute the pixels. This gives X-rays a slightly darker appearance. This process produces a vision that radiologists wouldn't typically see at work. X-ray images were stain-normalized using the Reinhard and Macenko methods [21-23].

B) Feature extraction stage

The commonly utilized "deep neural networks" in machine vision, such as CNN, are found to be analogous to multi-layer perceptrons (MLP). The distinction lies in its ability to integrate several "locally connected" layers for feature extraction with several "fully connected" layers employed in the classification process [24]. CNNs are effective for tasks such as object identification, image recognition, and visualization. In the realm of AI and deep learning, CNNs are extensively used, particularly in medical image processing. One of their notable advantages is their ability to analyze large datasets without the need for manual feature extraction. Moreover, they eliminate the necessity for intricate segmentation processes [25]. CNNs use a matrix of pixel values as opposed to feed forward neural networks (FFNs), which take in a vector of pixel values. Shared weights, which are a collection of connections that share the same weights rather than utilizing a different weight for each link, are one of the most advantageous characteristics of CNNs. The local connection is another characteristic; not every neuron communicates with every neuron in the layer above it. Instead of contacting all cells, it just makes contact with a certain group of neurons to determine whether they possess the feature of the object. This topic causes a lot of discussion because it is necessary to extract local features from an image input (such ridges, edges, and curves). The amount of parameters in the network is greatly reduced by these two characteristics, which shortens the training period[25]. The CNN's basic design is made up of three unique levels, and any CNN model is built utilizing these layers [26]:

- Convolution layer

The filter set (kernel) for this layer is present. The input image is subjected to each filter, convolved, and features are then retrieved by generating a new layer. One or more of the most essential characteristics or features of the input image are represented by each layer. The convolution's mode of operation is indicated by the * symbol. When input $I_n(t)$ is convolved with a filter or $F(a)$, kernel, the result, or function map, $F(t)$, described below.

$$F(t) = (I_n * f)(t) \quad (1)$$

The next discrete convolution is produced by the next equation if t can only accept integer values:

$$F(t) = \sum I_n(a) \cdot f(t - a) \quad (2)$$

The preceding assumes a convolutional operation in one dimension. With input $I_n(m, n)$ and a kernel $f(a, b)$, a two-dimensional convolution process is defined as:

$$F(t) = \sum_a \sum_b I_n(a, b) \cdot f(m - a, n - b) \quad (3)$$

The kernel is reversed by the commutative law, and the preceding is equivalent to:

$$F(t) = \sum_a \sum_b I_n(m - a, n - b) \cdot f(a, b) \quad (4)$$

The cross-correlation function, which is similar to convolution but doesn't flip the kernel, is implemented by neural networks.

$$F(t) = \sum_a \sum_b I_n(m + a, n + b) \cdot f(a, b) \quad (5)$$

- Rectified Linear Unit (ReLU) layer

The training and analysis are optimized and accelerated while also helping to maintain the gradient's visibility thanks to this layer's activation function, which lowers the negative input value to zero. In mathematics, this is represented as:

$$R(x) = \max(0, x) \quad (6)$$

Where x is the neuron's input.

- Maxpooling layer

A sample-based discretization technique is used in this Layer. By downsampling and reducing the dimensionality of an input design (input image, hidden layers, output matrix, etc.), assumptions can be made about the components that are present in the binned sub-regions. As a result, the number of the learning parameters will be reduced and the internal depiction will have fundamental interpretation invariance, further lowering computation costs. During the Maxpooling procedure, our model adopted a kernel size of 3×3 . The network collapsed to one dimension after the last convolution block.

Between the dropout layers and the convolutional layers is a technique called max-pooling. Use of the dropout layer is at a low ratio of (0.1). Convolutional and ReLU layers, max-pooling layers, and dropout layers, in that order, make up one of the five blocks in the suggested architectural architecture for CNN. Its primary goal is to minimize the dimensions by scaling down the activation map to a fourth of its original size while retaining the most crucial information[27].

C) Classification stage

Fully connected layers, the final layers of the CNN structure, it works as a classifier to determine the likelihood that an object is present in the image using the Softmax function in the output layer.

- SoftMax classifier

The architecture includes a dense layer of fully connected neurons with a ReLU activation function after the flattened layer resembling the CNN structure. A dropout layer with a ratio of 0.4 is employed to regulate and prevent overfitting. The output layer, Dense Layer 2, serves for COVID-19 diagnosis. The Softmax activation function processes the output to determine category probabilities based on the input CT image. The probabilities from Dense Layer 2 are fed into the loss function (equation 7) to calculate the error value for updating weights during the backpropagation process in training [28].

$$\text{loss} = - \sum_{c=1}^M (y_c \cdot \log \hat{y}_c) \quad (7)$$

Where \hat{y}_c is the model's forecast for that class (i.e., the output of the softmax for class c and M is the number of classes. Given that y is a (1000×1) vector of ones and zeroes and that the labels are one-hot encoded, y_c is either 1 or 0. Thus, only the term with $y_c = 1$ will really be added to the total amount.

In the subsequent stage, chest x-ray images undergo multiple passes on the CNN structure in both forward and backward directions. This process is governed by early stopping to minimize the error (loss) between the actual label of the training sample and the predicted output of the CNN model. The weights are adjusted during this process, and a set of trained weights and kernels for each layer in the network architecture is obtained through CNN training. These training weights are stored for later use by the network in the testing phase.

During the test phase of the CNN, evaluations are conducted on unseen test data. The initial step in the test algorithm involves pre-processing. In the test phase, chest X-ray images undergo forward propagation through the CNN structure to extract features. These images are then classified into categories such as COVID-19, healthy, pneumonia, and lung opacity. The classification is done using the trained weights in the "fully connected" layers and the trained kernel in the convolution layer. These weights and kernels were saved during the training phase and utilized in the test phase for accurate classification.

- Classification performance analysis

The confusion matrix predicts the four following results. The correct diagnosis and a number of anomalies have allowed for the identification of True Positives (TP). An incorrectly computed number of periodic occurrences are known as True Negative (TN). False positives (FP) are a collection of recurring events. The matrix's components are used to assess the model's precision, recall, F1 score, negative predicted values, and specificity[29]. Accuracy in Equation (8) is the percentage of COVID-19, normal, pneumonia, and lung opacity cases from all samples that were accurately recognized.

$$\text{Accuracy} = \frac{TP+TN}{TP+TN+FP+FN} \quad (8)$$

Precision, also known as positive predicted value (PPV) is the percentage of samples in Equation (9) that were properly identified.

$$\text{Precision} = \frac{TP}{TP+FP} \quad (9)$$

Sensitivity or recall is the proportion of correctly identified cases to all correctly detected but incorrectly classified cases, or all of the original samples in Equation (10).

$$\text{Recall} = \frac{TP}{TP+FN} \quad (10)$$

The F1 score in Equation (11) represents the model's overall accuracy score taking precision and recall into account.

$$F1 - \text{Score} = 2 \left(\frac{\text{Precision} \times \text{Recall}}{\text{Precision} + \text{Recall}} \right) \quad (11)$$

Negative predicted value (NPV) in Equation (12) refers to the proportion of correctly diagnosed cases across all samples.

$$NPV = \frac{TN}{TN+FN} \quad (12)$$

Specificity The ratio of correctly identified cases to the total number of correctly and incorrectly identified cases which defined in Equation (13).

$$\text{Specificity} = \frac{TN}{TN+FP} \quad (13)$$

Fig .3 shows the confusion matrix for making a diagnosis using chest x-ray images. Table 2 lists the basic evaluation metrics for making a diagnosis using chest x-ray images.

		Confusion Matrix			
		COVID	Lung_opacity	Normal	Pneumonia
True Class	COVID	479	2	3	1
	Lung_opacity	3	468	5	1
	Normal	4	3	436	1
	Pneumonia	2		2	457
		Predicted Class			

Fig .3 Confusion matrix for diagnosing based on chest x-ray images.

Table 2 lists the basic evaluation metrics for diagnosing based on chest x-ray images.

Class Name	TP	TN	FP	FN	Precision	Sensitivity	Specificity	F-measure
COVID	479	1373	9	6	0.98	0.99	0.99	0.98
Normal	436	1413	10	8	0.98	0.98	0.99	0.98
Pneumonia	457	1403	3	4	0.99	0.99	1.00	0.99
Lung opacity	468	1385	5	9	0.99	0.98	1.00	0.99
Average					0.99	0.99	1.00	0.99

From the basic evaluation metrics shown in table 2, the accuracy is 0.99%, the error value is 0.01% and the NPV is 1.00%.

3.2. Diagnosing Based on Medical Analysis Laboratory Data Findings

The blood test results which determine whether the case is infected with the coronavirus or not, is extremely crucial to the diagnosis process and detection of suspected cases of COVID-19. So, the blood tests most indicative of infection with the coronavirus were chosen, such as white blood cell (WBC), D-dimer, lymphocytes, and C-reactive protein (CRP). D-dimer test is a blood test that looks for issues with blood coagulation. Its rise is typically noticed in individuals with acute COVID-19 because to the condition's common thromboembolic consequences or acute lung injury itself[30]. A test called WBC count counts the WBCs in a sample of blood. This number is a crucial indicator of inflammation. Increased counts (more than 11,000 WBCs per unit microliter of blood) may affect COVID-19 patients' hospital release rates and mortality rates[31]. Due of an inflammatory response and associated tissue degradation, coronavirus appears to considerably raise CRP levels. This was also observed in the SARS pandemic of 2002. More severe disease that is associated with lung damage is indicated by higher amounts[32]. Many of researches suggest that people with COVID-19 frequently have lymphopenia, which is characterized by a low lymphocyte count [33, 34].Table 3 shows the main laboratory findings [35-38].

Table 3 the main laboratory findings.

Laboratory finding	Normal range	COVID-19 group
D-dimer (mg/L)	≤ 0.5	0.5 $\mu\text{g/mL}$ to more than 10 000 $\mu\text{g/mL}$
(WBC)	4,500 to 11,000 WBCs /ml	>11000 m/l
CRB	≤ 3.0 mg/L	30–50 mg/L
lymphocytes	Between 800 and 5000 (0.8-5.0) lymphocytes per mL of blood	<800 per mL of blood

3.3. Diagnosing Based on Symptoms

There are many symptoms that often appear in people infected with the Corona virus, such as: fatigue fever, sore throat, breathlessness, cough, and malaise among others. In our proposed system, some of

these symptoms such as fever, cough, cough with sputum, smell or loss of taste, shortness of breath, and headache. They were selected according to what was mentioned on the WHO website[39], and according to what was also reported in many researches[40-44].

4. Applications and Experimental Results

4.1. Description of the Proposed System

The proposed system for detecting of suspected cases of COVID-19 is designed using Python 3.11 and Matlab R2023b as programming languages. Figure 4 depicts the suggested system's graphical user interface (GUI). As shown in fig.4 the proposed system GUI includes four tabs: the first called "Diagnosing using X-ray images". The button "Load image" for selecting any chest X-ray images from any class "COVID-19, normal, pneumonia, and lung opacity". Then pressing the button "analyze" to give the decision "COVID-19, or normal, or pneumonia, or lung opacity", this decision takes 25%.

The second tab called "Diagnosing using laboratory findings" shown in Fig.5. Laboratory values are written in text boxes, and based on the entered values and according in Table 3, the case is classified as whether it is infected with the COVID-19 or normal. Each laboratory data takes 15%.

The third tab called "Diagnosing using clinical symptoms" shown in fig.6.

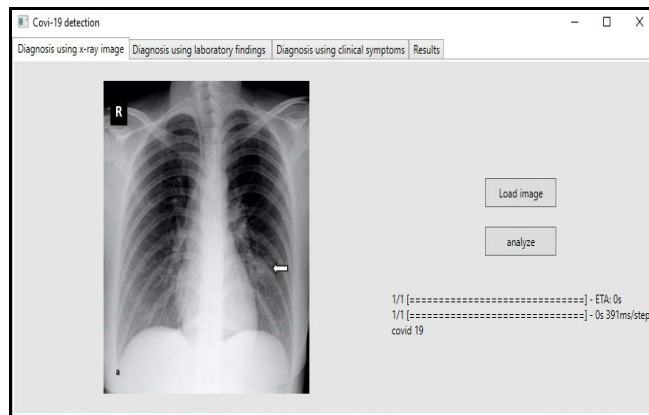


Fig.4 The proposed system GUI, first tab.

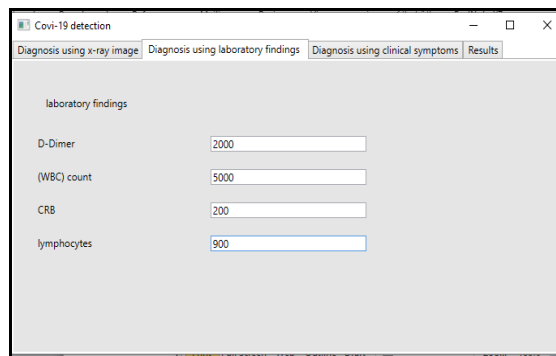


Fig.5 The proposed system GUI, second tab.

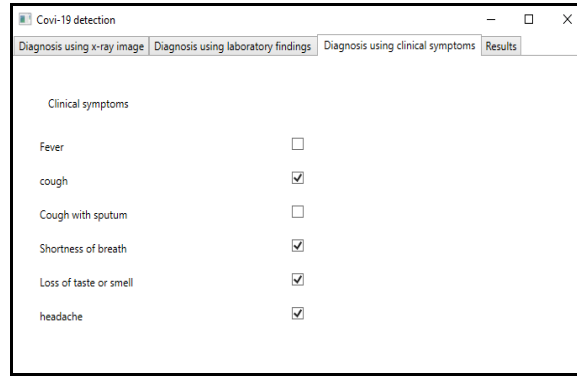


Fig.6 The proposed system GUI, third tab.

It consists of the main clinical symptoms which if selected any of them; the person will be classified as having coronavirus, and if no symptom is selected, the person will be classified as normal. Each clinical symptom takes 2.5%.

The fourth tab called “results” shown in fig.7. It shows the final decision for the three decisions of diagnosing in ratio for healthy or normal and COVID-19, when pressing the button “calculate”; where the final decision is made by the largest percentage.

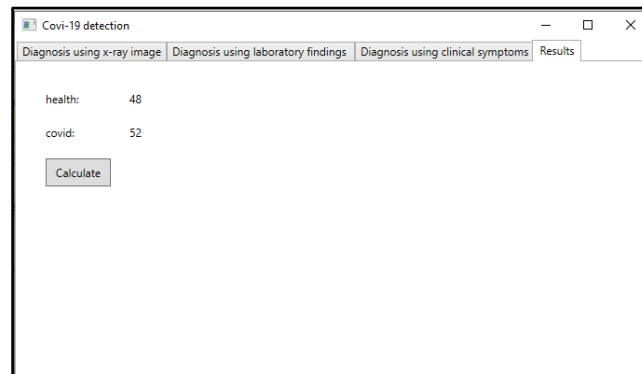


Fig.7 The proposed system GUI, fourth tab.

4.2.Evaluation of the Proposed System

For testing and evaluating the system, 30 files were taken of cases diagnosed by doctors at Chest Diseases Hospital, Mansoura University. We entered the cases data, including chest X-ray images, laboratory analyzes and symptoms, in the proposed system, and compared its results with the experts’ diagnosis; It was found that the proposed system produced high accuracy and efficiency in diagnosis at a rate of 0.97% with error value 0.03% and the NPV 0.97%; and this qualifies the proposed system to help students or doctors of medical institutions in quickly diagnosing cases suspected of being infected with the coronavirus or its variants. Fig.8 shows the confusion matrix for testing data for the proposed intelligent educational system. And Table 4 shows the essential evaluation metrics for testing data for the proposed intelligent educational system.

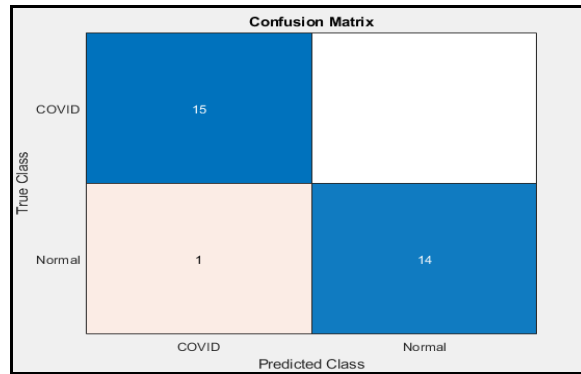


Fig.8 The confusion matrix for testing data for the proposed intelligent educational system

Table 4 lists the basic evaluation metrics for testing data for the proposed intelligent educational system.

Class Name	TP	TN	FP	FN	Precision	Sensitivity	Specificity	F-measure
COVID	15	14	1	0	0.94	1.00	0.93	0.97
Normal	14	15	0	1	1.00	0.93	1.00	0.97
Average					0.97	0.97	0.97	0.97

5. Conclusions and Future Work

COVID-19 is now a pandemic that spreads rapidly through both direct and indirect human contact. Manual temperature measuring and disinfection techniques are used in homes and public places, however they may help the COVID-19 disease spread. Even though we must acknowledge that this sickness will continue to affect us moving forward, we must nonetheless exercise extreme caution to prevent its spread.

The proposed system can be used to validate medical professionals' judgments. The system achieves great precision, which boosts its effectiveness and applicability for application, according to the experimental results. Previous research has concentrated on images or laboratory data, while others have focused on symptoms for the detection procedure. Whereas the proposed system is more distinct and exceptional due to its capacity to integrate laboratory data and images and symptoms into only one system for detecting process, additionally due to its diversity in the use of methodologies, algorithms, and design tools.

The proposed system can classify COVID-19, normal, pneumonia, and lung opacity cases and has a high accuracy rate of 0.97%. Although it has a simple architecture, is computationally efficient, and produces good results, its sensitivity could be improved any more if more reliable radiologist data were available. One of the advantages of the proposed system; it can be applied in any medical institution, not only in medical educational institutions. Future work can enhance the system's efficacy by including the patient's chest sound in addition to chest x-ray images, symptoms, and laboratory data to help in the detection process.

Acknowledgments The authors express their gratitude for the support provided by the Department of Chest Diseases and the Department of Radiology at Mansoura University Hospital in Mansoura, Egypt.

References

1. ÇINARER, G. and K. KILIÇ, *Investigation of Deep Learning Algorithms for COVID-19 Detection Based on Chest X-ray Images*. Artificial Intelligence Theory and Applications, 2021. **2**: p. 280-287.
2. Li, Y., et al., *Stability issues of RT-PCR testing of SARS-CoV-2 for hospitalized patients clinically diagnosed with COVID-19*. J Med Virol, 2020. **92**(7): p. 903-908. <https://doi.org/10.1002/jmv.25786>
3. Kanji, J.N., et al., *False negative rate of COVID-19 PCR testing: a discordant testing analysis*. Virology journal, 2021. **18**(1): p. 1-6. <https://doi.org/10.1186/s12985-021-01489-0>
4. Abdleall, N., A. Elalfi, and F.A.E.-S. Zahran El-Mougi, *An Intelligent Educational System for Breast Cancer Management*. International Journal of Intelligent Computing & Information Sciences, 2022. **22**(3). <https://dx.doi.org/10.21608/ijicis.2022.136628.1179>
5. Borchers, A. and T. Pieler, *Programming pluripotent precursor cells derived from Xenopus embryos to generate specific tissues and organs*. Genes (Basel), 2010. **1**(3): p. 413-26. <https://doi.org/10.3390/genes1030413>
6. Abd El-badie Abd Allah, A. and F.A.E.-S.Z. El, *A Fuzzy Decision Support System for Diagnosis of Some Liver Diseases in Educational Medical Institutions*. International Journal of Fuzzy Logic and Intelligent Systems, 2020. **20**(4): p. 358-368. DOI: [10.5391/IJFIS.2020.20.4.358](https://doi.org/10.5391/IJFIS.2020.20.4.358)
7. M, V.M., et al., *Detection of COVID-19 Using Deep Learning Techniques and Cost Effectiveness Evaluation: A Survey*. Front Artif Intell, 2022. **5**: p. 1-16. <https://doi.org/10.3389/frai.2022.912022>
8. Mathieu, E., et al., *A global database of COVID-19 vaccinations*. Nat Hum Behav, 2021. **5**(7): p. 947-953. DOI: <https://doi.org/10.1038/s41562-021-01122-8>
9. Shi, F., et al., *Review of Artificial Intelligence Techniques in Imaging Data Acquisition, Segmentation, and Diagnosis for COVID-19*. IEEE Rev Biomed Eng, 2021. **14**: p. 4-15. DOI: [10.1109/RBME.2020.2987975](https://doi.org/10.1109/RBME.2020.2987975)
10. Morimoto, S., et al., *aPDT for oral decontamination of hospitalized patients with COVID 19*. Photodiagnosis Photodyn Ther, 2022. **38**: p. 102762. <https://doi.org/10.1016/j.pdpdt.2022.102762>
11. Xia, M., et al., *Fault diagnosis for rotating machinery using multiple sensors and convolutional neural networks*. IEEE/ASME transactions on mechatronics, 2017. **23**(1): p. 101-110. DOI: [10.1109/TMECH.2017.2728371](https://doi.org/10.1109/TMECH.2017.2728371)
12. El Fiky, A.H., *Deep COVID 19: Deep Learning for COVID 19 Detection from X ray Images*. International Journal of Innovative Technology and Exploring Engineering, 2021. **11**(1): p. 1-6. DOI: [10.35940/ijitee.A9589.1111121](https://doi.org/10.35940/ijitee.A9589.1111121)
13. Reshi, A.A., et al., *An Efficient CNN Model for COVID-19 Disease Detection Based on X-Ray Image Classification*. Complexity, 2021. **2021**: p. 1-12. <https://doi.org/10.1155/2021/6621607>
14. Ahmed, Z.S., et al., *CNN-based Transfer Learning for Covid-19 Diagnosis*. 2021: p. 296-301. DOI: [10.1109/ICIT52682.2021.9491126](https://doi.org/10.1109/ICIT52682.2021.9491126)
15. Shah, F.M., et al., *A Comprehensive Survey of COVID-19 Detection Using Medical Images*. SN Comput Sci, 2021. **2**(6): p. 1-22. DOI: [10.1007/s42979-021-00823-1](https://doi.org/10.1007/s42979-021-00823-1)

16. Wang, L., Z.Q. Lin, and A. Wong, *COVID-Net: a tailored deep convolutional neural network design for detection of COVID-19 cases from chest X-ray images*. Sci Rep, 2020. **10**(1): p. 19549. <https://doi.org/10.1038/s41598-020-76550-z>
17. Available at: <https://www.kaggle.com/datasets/tawsifurrahman/tuberculosis-tb-chest-xray-dataset>, date of access: 23/9/2023
18. Available at: <https://www.kaggle.com/datasets/tawsifurrahman/covid19-radiography-database>, date of access: 21/6/2023.
19. Available at: <https://www.kaggle.com/datasets/prashant268/chest-xray-covid19-pneumonia>, date of access: 21/6/2023.
20. Campos, G.F.C., et al., *Machine learning hyperparameter selection for contrast limited adaptive histogram equalization*. EURASIP Journal on Image and Video Processing, 2019. **2019**: p. 1-18. <https://doi.org/10.1186/s13640-019-0445-4>
21. Deif, M.A., et al., A hybrid multi-objective optimizer-based SVM model for enhancing numerical weather prediction: A study for the Seoul metropolitan area. Sustainability, 2021. **14**(1): p. 296. <https://doi.org/10.3390/su14010296>
22. Macenko, M., et al. A method for normalizing histology slides for quantitative analysis. in 2009 IEEE international symposium on biomedical imaging: from nano to macro. 2009. IEEE. DOI: [10.1109/ISBI.2009.5193250](https://doi.org/10.1109/ISBI.2009.5193250)
23. Tan, M. and Q. Le. *Efficientnet: Rethinking model scaling for convolutional neural networks*. in *International conference on machine learning*. 2019. PMLR. <https://doi.org/10.48550/arXiv.1905.11946>
24. Al-Waisy, A.S., et al., *A multi-biometric iris recognition system based on a deep learning approach*. Pattern Analysis and Applications, 2018. **21**: p. 783-802. <https://doi.org/10.1007/s10044-017-0656-1>
25. Heidari, J., *Classifying Material Defects with Convolutional Neural Networks and Image Processing*. 2019.
26. Sarki, R., et al., *Automated detection of COVID-19 through convolutional neural network using chest x-ray images*. Plos one, 2022. **17**(1): p. e0262052. <https://doi.org/10.1371/journal.pone.0262052>
27. Gong, W., et al., A novel deep learning method for intelligent fault diagnosis of rotating machinery based on improved CNN-SVM and multichannel data fusion. Sensors, 2019. **19**(7): p. 1693. <https://doi.org/10.3390/s19071693>
28. Raghu, M., et al., *Transfusion: Understanding transfer learning for medical imaging*. Advances in neural information processing systems, 2019. **32**.
29. Akter, S., et al., *COVID-19 detection using deep learning algorithm on chest X-ray images*. Biology, 2021. **10**(11): p. 1174. <https://doi.org/10.3390/biology10111174>
30. Lehmann, A., et al., *Impact of persistent D-dimer elevation following recovery from COVID-19*. PLoS One, 2021. **16**(10): p. e0258351. <https://doi.org/10.1371/journal.pone.0258351>
31. Zhu, B., et al., *Correlation between white blood cell count at admission and mortality in COVID-19 patients: a retrospective study*. BMC infectious diseases, 2021. **21**: p. 1-5. <https://doi.org/10.1186/s12879-021-06277-3>
32. Alabd, S.F. and A.A. Yameny, *C-Reactive Protein as a Prognostic Indicator in COVID-19 mild infection Patients*. Journal of Medical and Life Science, 2021. **3**(2): p. 38-43. DOI: [10.21608/jmals.2021.240126](https://doi.org/10.21608/jmals.2021.240126)
33. Guan, W.-j., et al., *Clinical characteristics of coronavirus disease 2019 in China*. New England journal of medicine, 2020. **382**(18): p. 1708-1720.
34. Terpos, E., et al., *Hematological findings and complications of COVID-19*. American journal of hematology, 2020. **95**(7): p. 834-847. <https://doi.org/10.1002/ajh.25829>

35. Manoharan, L., et al., *Early clinical characteristics of Covid-19: scoping review*. MedRxiv, 2020: p. 2020.07.31.20165738. DOI: <https://doi.org/10.1101/2020.07.31.20165738>
36. Terra, P.O.C., et al., Neutrophil-to-lymphocyte ratio and D-dimer are biomarkers of death risk in severe COVID-19: a retrospective observational study. *Health Science Reports*, 2022. **5**(2): p. e514. <https://doi.org/10.1002/hsr2.514>
37. Pourbagheri-Sigaroodi, A., et al., *Laboratory findings in COVID-19 diagnosis and prognosis*. *Clinica chimica acta*, 2020. **510**: p. 475-482. <https://doi.org/10.1016/j.cca.2020.08.019>
38. Ghahramani, S., et al., Laboratory features of severe vs. non-severe COVID-19 patients in Asian populations: a systematic review and meta-analysis. *European journal of medical research*, 2020. **25**(1): p. 1-10.
39. Organization, W.H. https://cdn.who.int/media/images/default-source/health-topics/coronavirus/covid19-infographic-symptoms-final.png?sfvrsn=57850cbc_6. May 2023.
40. Mousa, H.A., *Prevention and treatment of COVID-19 infection by earthing*. *Biomed J*, 2023. **46**(1): p. 60-69. <https://doi.org/10.1016/j.bj.2022.08.002>
41. Hafeez, A., et al., A review of COVID-19 (Coronavirus Disease-2019) diagnosis, treatments and prevention. *Ejmo*, 2020. **4**(2): p. 116-125.
42. Clemency, B.M., et al., *Symptom criteria for COVID-19 testing of health care workers*. *Academic Emergency Medicine*, 2020. **27**(6): p. 469-474.
43. Salman, F.M. and S.S. Abu-Naser, *Expert system for COVID-19 diagnosis*. 2020. <https://doi.org/10.1111/acem.14009>
44. Alimohamadi, Y., et al., *Determine the most common clinical symptoms in COVID-19 patients: a systematic review and meta-analysis*. *Journal of preventive medicine and hygiene*, 2020. **61**(3): p. E304. DOI:[10.15167/2421-4248/jpmh2020.61.3.1530](https://doi.org/10.15167/2421-4248/jpmh2020.61.3.1530)